

**PREPARATION AND CHARACTERIZATION OF Al-SUBSTITUTED  
M-TYPE FERRITES BY SOL-GEL AUTO COMBUSTION METHOD**

*A Dissertation submitted in fulfillment of the requirements for the Degree*

*Of*

**MASTER OF SCIENCE**

*In*

**Physics**

Submitted by

**Reena Rani**

**(Roll no. 301504028)**

Under the supervision of

**Dr. Puneet Sharma**

Associate Professor, SPMS



**School of Physics & Material Science**

**Thapar University, Patiala- 147004**

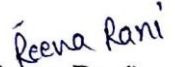
**Punjab (India)**

**July, 2017**

## CERTIFICATE


I hereby certify that the work which is being presented in this report entitled, "PREPARATION AND CHARACTERIZATION OF AI-SUBSTITUTED M-TYPE FERRITES BY SOL-GEL AUTO COMBUSTION METHOD" as a part of curriculum during Master of Science in Physics, submitted to School of Physics & Material Science of Thapar University, Patiala, is an authentic record of my own work carried under the supervision of Dr. Puneet Sharma, SPMS. It refers others researcher's work which are duly listed in the reference section. The matter contained in this report has not been submitted, neither in part or in full to any other degree to any other university or institute except as reported in text and references.

Place: Patiala  
Date: 17<sup>th</sup> July, 2017

  
(Reena Rani)  
Roll No: 301504028

This is to certify that the above mentioned statement of the student is correct to the best of my knowledge and belief.

Date: 17<sup>th</sup> July, 2017

  
Dr. Puneet Sharma  
Associate Professor  
School of Physics & Material Science  
Thapar University, Patiala

## ACKNOWLEDGEMENT

---

I would like to thank **Dr. Puneet Sharma**, Associate Professor (SPMS), for giving me a chance to work under his supervision, without whose help and constant guidance this thesis would have not taken shape. I am extremely thankful to **Dr. O. P. Pandey**, Dean of Research, for their cooperation and encouragement. I am also thankful to all staff members of SPMS, for their constant cooperation in experimental work.

I am highly thankful to my senior PhD scholar **Mr. Santhosh Kumar Mahadevan, Ms. Chhavi Pahwa, Ms. Shivani Jindal, and Mr. Anoop Partap Singh** who provided their valuable guidance and suggestions during the course of the work. I acknowledge and thank my elders and my relatives for their support and motivation. I am very thankful to my parents and my brother for their constant cooperation, inspiration, patience, blessing and moral support.

*Reena Rani*  
**Reena Rani**

**(301504028)**

## TABLE OF CONTENTS

---

Certificate	ii
Acknowledgement	iii
Table of Contents	iv
List of Tables	vi
List of Figures	vii
Abstract	viii
<b>CHAPTER 1: INTRODUCTION</b>	<b>1-10</b>
1.1 Introduction	1
1.2 Types of Hexaferrite	2-3
1.2.1 M- Type Hexaferrite	1
1.2.2 W-Type Hexaferrite	2
1.2.3 X- Type Hexaferrite	2
1.2.4 Y- Type Hexaferrite	3
1.2.5 Z- Type Hexaferrite	3
1.2.6 U- Type Hexaferrite	3
1.3 Crystal Structure and Magnetic Structure of M- Type Hexaferrite	4
1.4 Intrinsic properties of M- Type Hexaferrite	6
1.5 Processing method	6
1.6 Sol-Gel auto combustion Method	6
1.7 Application of M- Type Hexaferrite	7
1.8 Motivation and Objective of the Thesis	8
1.9 Organization of the Thesis	9
<b>CHAPTER 2: LITREATURE REVIEW</b>	<b>10-15</b>
<b>CHAPTER 3: EXPERIMENTAL DETAIL</b>	<b>16-17</b>
3.1 Sample preparation	16

<b>CHAPTER 4: RESULT AND DISCUSSION</b>	<b>18-25</b>
4.1 X- Ray Diffraction (XRD)	18
4.2 Scanning Electron Microscopy (SEM)	20
4.3 Energy Dispersive Spectroscopy (EDS)	21
4.4 Magnetic properties	22
<b>CHAPTER 5: CONCLUSION AND FUTURE SCOPE</b>	<b>26</b>
<b>REFERENCES</b>	<b>27-32</b>

## LIST OF TABLES

---

Table no.	Title	Page No.
Table 1.1	Types of hexaferrite	1
Table 1.2	Crystallographic properties of M- Type hexaferrite	2
Table 1.3	Crystal and Magnetic structure of hexaferrite	6
Table 1.4	Primary and secondary properties of M-Type hexaferrite	6
Table 4.1	Calculated structural parameter of Al-substituted BaM and SrM	20
Table 4.2	Variation of particle size with aluminium substitution	21
Table 4.3	Element analysis for SrFe <sub>12</sub> O <sub>19</sub> and SrFe <sub>10</sub> Al <sub>2</sub> O <sub>19</sub>	22
Table 4.4	Magnetic properties of Al-substituted SrM and BaM powder	23
Table 4.5	<i>M-H</i> Behaviour of sintered fractured pellet of Al- substituted SrM and BaM	25

## LIST OF FIGURES

Figure No.	Title	Page No.
Figure 1.1	S and R block in hexagonal crystal structure	4
Figure 1.2	Crystal structure of M- Type Hexaferrite	5
Figure 1.3	Combustion powder	7
Figure 3.1	Flow chart for preparation of Al-substituted SrM	17
Figure 4.1	XRD patterns for (a) $\text{SrFe}_{12-x}\text{Al}_x\text{O}_{19}$ ( $x=0,1,2$ ) (b) $\text{BaFe}_{12-x}\text{Al}_x\text{O}_{19}$ ( $x=0,1,2$ )	19
Figure 4.2	SEM images of sintered fractured pellets of $\text{SrFe}_{12-x}\text{Al}_x\text{O}_{19}$ (a) $x = 0$ , (b) $x = 2$	20
Figure 4.3	EDS Spectrum of sintered fractured pellet $\text{SrFe}_{12-x}\text{Al}_x\text{O}_{19}$ (a) $x=0$ , (b) $x=2$	21
Figure 4.4	Magnetization curve of (a) $\text{SrFe}_{12-x}\text{Al}_x\text{O}_{19}$ ( $x=0,1$ ) (b) $\text{BaFe}_{12-x}\text{Al}_x\text{O}_{19}$ ( $x=0,1$ )	23
Figure 4.5	$M-H$ behavior of sintered fractured pellet (a) $\text{SrFe}_{12-x}\text{Al}_x\text{O}_{19}$ ( $x=0,1,2$ ) (b) $\text{BaFe}_{12-x}\text{Al}_x\text{O}_{19}$ ( $x=0,1,2$ )	24

## ABSTRACT

---

M-type ferrites especially barium and strontium ferrite has dominant position in permanent magnet market due to its high coercivity, moderate saturation magnetization and energy product. Apart from its application in permanent magnets, there are also useful for high frequency application due to its high anisotropic constant and ferromagnetic resonance frequency. In the present work,  $\text{BaFe}_{12-x}\text{Al}_x\text{O}_{19}$  and  $\text{SrFe}_{12-x}\text{Al}_x\text{O}_{19}$  ( $x=0, 1, 2$ ) sintered magnets have been prepared. The Al-substituted powders were prepared by sol-gel auto-combustion method. The structural, microstructural and magnetic properties of the powders and sintered magnets were measured by X-Ray diffraction, scanning electron microscopy, and Vibrating Sample Magnetometer respectively. It is found the Al substitution remarkably affects its magnetic properties. A very high coercivity of 10.70 kOe was observed in Al substituted sintered magnets. However, saturation magnetization was found to decrease with the substitution. These high coercivity magnets could be useful for permanent magnet application where large demagnetization fields are dominating.

# CHAPTER-1

## INTRODUCTION

---

### 1.1 Introduction

Ferrites are very important due to its technological applications in permanent magnets, microwave, and magnetoelectric devices etc. [1]. Ferrites can be classified on the basis of their magnetic behavior, i.e. magnetically soft and hard ferrites. Magnetically soft ferrites, which include spinel and garnets, are important for high frequency application. Whereas, magnetically hard with hexagonal structure are used as permanent magnets and microwave devices above 50 GHz. These hexagonal ferrites are basically classified into six major types on the basis of their chemical formulae and crystal structure, tabulated in table 1.1 [2]. The crystal structures of these hexaferrites can be described by stacking the sequences of basic blocks: S (Spinel block), R [(Ba, Sr) Fe<sub>6</sub>O<sub>11</sub>]<sup>2-</sup>, and T [(Ba, Sr)<sub>2</sub>Fe<sub>8</sub>O<sub>14</sub>]. Among the class of hexagonal ferrites, barium hexaferrite (BaFe<sub>12</sub>O<sub>19</sub>), or BaM become massively important due to its high permeability (necessarily >1), high magnetization ( $M_s$ ), large magneto-crystalline anisotropy, high coercivity ( $H_c$ ), high Curie temperature and low dielectric losses [3]. Due to its tailorable properties these materials are widely employed as radar absorbing materials [4], permanent magnets, and magnetic recording media (data storage devices) etc.

**Table 1.1** Type of Hexaferrite

Type	Formula	Example
<b>M-</b>	MFe <sub>12</sub> O <sub>19</sub>	M= Ba, Pb, Sr
<b>W-</b>	MR <sub>2</sub> Fe <sub>16</sub> O <sub>27</sub>	R= Fe <sup>2+</sup> , Ni <sup>2+</sup> , Zn <sup>2+</sup> etc.
<b>X-</b>	MRFe <sub>28</sub> O <sub>46</sub>	
<b>Y-</b>	M <sub>2</sub> R <sub>2</sub> Fe <sub>12</sub> O <sub>22</sub>	
<b>Z-</b>	M <sub>3</sub> R <sub>2</sub> Fe <sub>12</sub> O <sub>41</sub>	
<b>U-</b>	M <sub>4</sub> R <sub>2</sub> Fe <sub>36</sub> O <sub>60</sub>	

Substitution has leads tailorable properties which influence magnetic properties like  $M_s$ ,  $M_r$ ,  $H_c$  and  $H_a$  of hexaferrite.

## 1.2 Types of Hexaferrite

### 1.2.1 M-type hexaferrite

$MFe_{12}O_{19}$  which generally known as M-type hexaferrite due to its hexagonal crystal structure in which M generally IIA group elements such as Ca/Sr/Ba/Pb. M-type hexaferrite has a wide range of applications due to its magnetic properties, high performance to cost ratio, corrosion resistance, and chemical stability. These can be used as permanent magnets, components in magneto optical devices, microwaves, and high density magnetic recording media etc. [5]

The density, molecular mass and other properties have been described in Table 1.2.

**Table 1.2** Crystallographic properties of M-Type Hexaferrite

X-Ray parameters		BaM	SrM
Lattice Parameter (Å°)	<i>a</i>	5.89	5.86
	<i>c</i>	23.17	23.03
Density (g/cc)		5.29	5.10
Molecular weight (g)		1112	1062

### 1.2.2 W-type hexaferrite

W-type ferrites have  $MR_2Fe_{16}O_{27}$  as its formula where R can be  $Fe^{2+}$ ,  $Ni^{2+}$ ,  $Zn^{2+}$  etc. and M can be Ca, Sr, Ba and Pb. W-type hexaferrite have various applications, e.g.  $BaCo_{2x}Zn_xFe_{16}O_{27}$  is used to absorb the electromagnetic radiations in the microwave region, or non-conductive permanent magnets, in the magnetic refrigerators with respect to the zinc concentration x in the formula [6]. Hardness of W-type ferrites has been calculated as 5.5 GPa with respect to c axis [7] and density as  $5.31\text{gcm}^{-3}$ [8]. Ferrites which are RE-substituted usually have lesser matching thickness but the bandwidth is larger, in comparison to those which are not substituted [9].

### 1.2.3 X-type hexaferrite

The structure of X-type hexaferrite is related to the structure of M-type and W-type hexaferrite as they are formed by the superimposition of M-type and W-type structures [10]. They have the chemical formula as  $MRFe_{28}O_{46}$ , where R can be  $Fe^{2+}$ ,  $Ni^{2+}$ ,  $Zn^{2+}$  etc. and M can be Ba, Pb, Sr, etc.  $Fe_2$ -X compounds have better chemical stability as compared to  $Fe_2$ -W compounds with some technological applications like permanent magnets. The magnetic properties of these

hexaferrites depend on the divalent cations and the way of their distribution among the sub lattices. The density of the X- hexaferrite has been recorded as  $5.29 \text{ g cm}^{-3}$  [8].

#### 1.2.4 Y-type hexaferrite

Y-hexaferrite have general formula  $M_2R_2Fe_{12}O_{22}$ . They have excellent properties like high cut off frequency, low sintering temperature, etc. The Y-type hexaferrite have applications in the new types of chip components like multi-layer chip beads and inductors in high frequency range. Among the Y-hexaferrite,  $Zn_2Y$  has large permeability and low magnetic losses. Due to these interesting properties it is widely used in high frequency devices [11]. The density of the Y type hexaferrite is  $5.40 \text{ g cm}^{-3}$  [8] and molecular mass is 1410 g.

#### 1.2.5 Z-type hexaferrite

Z-hexaferrite have formula  $M_3R_2Fe_{12}O_{41}$  where R can be  $Fe^{2+}$ ,  $Ni^{2+}$ ,  $Zn^{2+}$  etc. and M can be Ba, Pb, Sr, etc. Z-type hexaferrite are member of hexaferrite family known as ferroplana. In this family of hexaferrite, at the room temperature, easy magnetization direction lies in the c-plane of the hexagonal structure [8]. Due to in plane anisotropy this ferrite behave like soft ferrite. This hexaferrite widely used in induction cores, and absorbers of electromagnetic noise. If  $Ba^{2+}$  is replaced by  $Sr^{2+}$ , the sintering temperature and partial pressure of oxygen can be lowered during the synthesis of  $Co_2Z$  type ferrites [12]. The frequency of permeability gets improved by this substitution but if  $Ba^{2+}$  is fully substituted, the permeability gets degenerated [12]. The density of the Z-type hexaferrite is  $5.35 \text{ g cm}^{-3}$  [8] and molecular mass is 2522 g.

#### 1.2.6 U-type hexaferrite

These hexaferrite have complex formula with higher oxygen represented as  $M_4R_2Fe_{36}O_{60}$  [13] having space group  $R_3-m$  can be described with the help of the sequence  $(RSR^*S^*TS)_3$  where \* symbol shows that there would be a rotation of  $180^\circ$  of the block about the c axis. The U-type hexaferrite is a new type of magneto electric material at room temperature. The densities of  $Co_2U$  and  $Zn_2U$  have been recorded as 5.44 and  $5.31 \text{ g cm}^{-3}$  [8] while its molecular mass is 3622 g.

The focus of the work in on M-Type hexaferrite, therefore the details of this ferrite are given below.

### 1.3 Crystal structure and magnetic structure of M-type ferrite

All the hexaferrites have very complex hexagonal crystal structure [14]. They all are closely related to each other. M, Y and S are the three combination ferrite which can be seen at simple level. Alelsklod has determined the M-type hexaferrite crystal structure. In major ferrite system, barium can be replaced by strontium and lead without too much distortion  $Me^{2+}$  and  $Fe^{3+}$  are smaller in size and interstitial sites between oxygen occupied by  $Fe^{3+}$ . In the hexaferrite, exist trigonal bipyramidal site containing R-block and in oxygen framework, octahedral and tetrahedral site are inhibited by divalent and trivalent ions.

The origin of hexagonal ferrite is from spinel ferrite. M-type hexaferrite have crystalline structure which can be described by stacking of  $SRS^*R^*$  blocks.

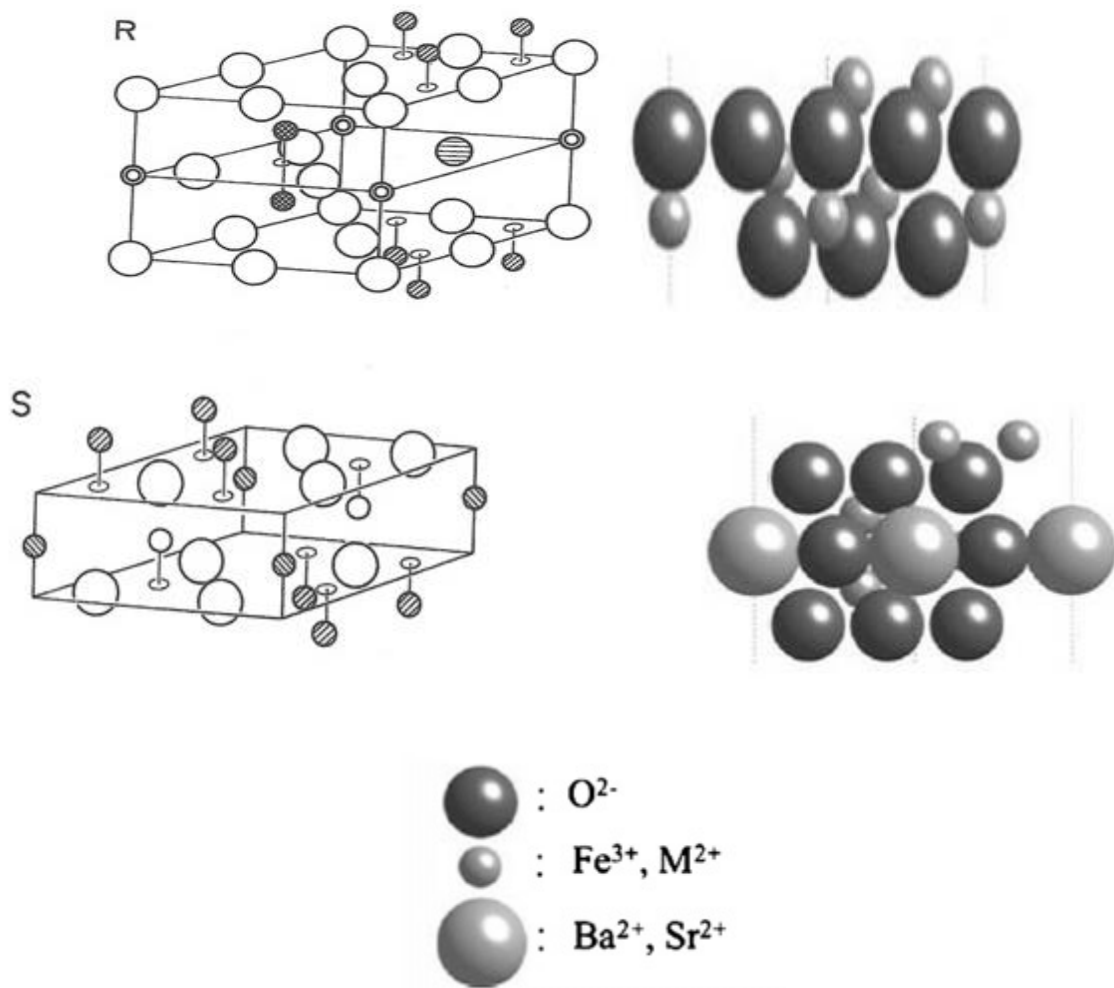


**Fig.1.1** S and R block in hexagonal crystal structure

- S block contains two spinel units ( $Me_2Fe_4O_8$ ) where Me is the divalent metal ion in which 4 oxygen atom in 2 layer of oxygen contain three metal atoms. Further, six oxygen anions are surrounded by cation in octahedral site and the cation surrounded by four oxygen anions in tetrahedral sites.

- In R block, four oxygen atoms consist in three hexagonal packed layers. Barium atom replaces one oxygen atom in center give  $\text{BaFe}_6\text{O}_{11}$  formula unit. The asymmetry creates by barium in cation site resulting five octahedral site, they pushed toward octahedral with bulky barium atom and five oxygen anions surrounded the cations in coordinate trigonal bipyramidal site.

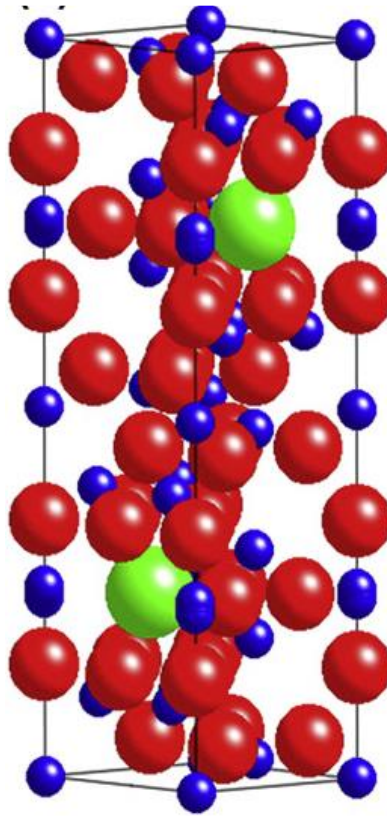


**Fig.1.2** Crystal structure of M -type hexaferrite

- Octahedral site ( $12k$ ,  $4f_2$ ,  $2a$ ), tetrahedral site ( $4f_1$ ), trigonal bipyramidal ( $2b$ ) are occupied by  $\text{Fe}^{3+}$  ion [15].

These  $\text{Fe}^{3+}$  ions have magnetic moment  $5\mu_B$  of each spin which spin up with total magnetic moment of  $40\mu_B$  per unit cell or  $20\mu_B$  per formula unit.

**Table 1.3** Crystal and magnetic structure [16]

Coordination	Sub lattice	No of ions	Spin
Tetrahedral	4f <sub>1</sub>	2	Down
Octahedral	12K	6	Up
Octahedral	4f <sub>2</sub>	2	Down
Octahedral	2a	1	Up
Trigonal bi-pyramidal	2b	1	Up

#### 1.4 Intrinsic property of M-type hexaferrite

The intrinsic properties of M- type hexaferrite are divided into two parts: primary and secondary. Primary properties like saturation magnetization and magneto crystalline constant are calculated from magnetic structure and secondary properties is determined from the primary one [17].

**Table 1.4** Primary and secondary properties of M-Type Hexaferrite [17]

<b>Primary properties</b>	
Saturation Magnetization, mT	475
Anisotropic constant, kJ/m <sup>3</sup>	360
Curie temperature, K	750
<b>Secondary properties</b>	
Specific wall energy, J/m <sup>2</sup>	54.2 x 10 <sup>-4</sup>
Anisotropy Field H <sub>A</sub> , kA/m	1506
Max Coercivity, (H <sub>c</sub> ) <sub>max</sub>	1240

#### 1.5 Processing method

Single phase barium hexaferrite can be synthesized by the following methods namely:

- Solid state method
- Sol-gel auto combustion
- Co-precipitation

In the next section, we will briefly explain the Sol-gel auto combustion technique to prepare the ferrite samples which we use in our present research work.

#### 1.6 Sol-gel auto combustion method

In materials science, the sol-gel is a process which allows mixing at an atomic level in which multi component compounds are prepared with a controlled stoichiometry. Among the available techniques, the sol-gel process is undoubtedly the simplest and the cheapest one. The method is used for the fabrication of metal oxides. The process involves conversion of monomers into a colloidal solution (*sol*) that acts as the precursor for an integrated network (or *gel*) of either discrete particles or network polymers. Typical precursors are metal alkoxides. Sol is a solution containing particles in suspension, is polymerized at low temperature to form a wet gel. This is going to be densified through a thermal annealing to give an inorganic product like a glass, polycrystals or a dry gel. After this, a thermal treatment or firing process is necessary for further ploycondensation. When we do the final sintering, we found enhance mechanical properties, structural stability, densification and grain growth [18].

### **Advantages of Sol-gel auto combustion Process**

1. Better homogeneity and phase purity compared to traditional ceramic method.
2. The sol-gel method prevents the problems with co-precipitation, which may be, inhomogeneous be a gelation reaction.
3. Enables mixing at an atomic level.
4. Results in small particles, which are easily sinterable.
5. Sol-gel derived materials have diverse applications in optics, electronics, energy, space etc. [19]



**Fig.1.3** Combustion powder

## 1.7 Application of M-Type hexaferrite

**1. Permanent magnet:** Alloys of rare earth metals especially neodymium is the best permanent magnet, but its manufacturing cost is too much high. For a good permanent magnet, a large saturation, remanence, coercivity and a large square loop with a high energy product is required [5]. Permanent magnets which are made from hard ferrites are not as good as alloys, but they are much easy and cheaper to make with all above mentioned features. Hence hard ferrites will become more attractive. M-Type hexaferrite as permanent magnets are used in loudspeakers, clocks, relay, magnetrons, electric motors, microphones, automobile, and refrigerator seal gaskets and in communication devices [5].

**2. Data storage Devices:** A square loop with a high remanence is required to store the data. However, for re-recording low coercivity is required, this can be tailored with varying substitution. BaM commercially used in audio tape, floppy disk and hard disk etc. [5]. In 2011 Fujifilm manufacture a tape using BaM particles, with storage capacity of 5TB and transfer speed of 240 MBs<sup>-1</sup>. One of such kind of tape can store 8 million books.

**3. Microwave Devices:** Hexaferrites are used in high frequency microwave devices like circulators, phase shifter, resonance isolators, and high speed digital electronics (like calculators, cell phones etc) [5]. The soft or hard ferrites can be needed according to applications. Microwave dielectric losses should be minimized for high microwave frequencies and wave absorbing material should have small thickness, light weight, wide absorption frequency range and absorption efficiency etc. [20]. Mostly hexaferrite have less eddy current losses due to high resistance so they are used in high frequency range such as radio especially raise the remanence. BaM is an excellent EM absorbing material in high frequency [21].

## 1.8 Motivation and Objective of the Thesis

In this thesis, the focus lies on the Al- substituted barium hexaferrite and strontium hexaferrite. BaM and SrM hexaferrite have been more attention due to significant application in permanent magnet and high frequency applications. Al-substituted in BaM/SrM modifies its magnetic properties such as coercivity, saturation magnetization. This might be widely useful for fabrication of permanent magnet which has high anisotropy field. Further, these trivalent ions improve the high frequency application of the hexaferrite material above 50GHz.

The main aim is to prepare the Al-substituted barium and strontium hexaferrite by sol-gel auto combustion route and to investigate its structural and magnetic properties.

## **1.9 Organization of the Thesis**

The effect of  $\text{Al}^{3+}$  substitution on the strontium and barium hexagonal ferrites has been investigated. The thesis is organized as follows.

In Chapter 2, summarizes the various important work carried out in past year on BaM and SrM. The magnetic behavior of BaM and SrM prepared by various processing techniques are listed. Effect of various ion substitution with an emphasize to  $\text{Al}^{3+}$  substitution on structural and magnetic properties has been reviewed.

In Chapter 3, the details of processing methodology, particularly sol-gel auto-combustion method are given. Further the details for various characterization tools used such as X- ray diffraction (XRD), Scanning Electron Microscopy (SEM), Energy Dispersive Spectroscopy (EDS), and Vibrating Sample Magnetometer (VSM) techniques were mentioned.

In Chapter 4, the obtained structural and magnetic properties are discussed in detail.

The thesis concludes in Chapter 5 where the work has been summarized and also some issues for further research have been discussed.

## CHAPTER-2

### LITERATURE REVIEW

---

Since the discovery of BaM and SrM by Philips laboratory, a tremendous amount of work has been carried out. The section below summarizes the important work based on their processing followed by various ion substitutions.

**In 1993**, C.Sürig studied the strontium hexaferrite and barium hexaferrite prepared by sol- gel technique with different Fe/Sr ratio. The saturation magnetization, coercivity, phase formation is found out from prepared single domain powder by two step heat treatment with high magnetization. Strontium has high coercive strength and magnetization as compared to barium ferrite. The phase formation and magnetic field strength of both is calculated by ferromagnetic resonance absorption at the time of heat treatment [22]. **In 1997**, Z.B.Guo reported strontium hexaferrite is synthesized by salt–melt method. He investigated the particle size, magnetic properties of SrM by using starting raw material  $\text{SrSO}_4$  with celestite. The result found that  $H_c$  has 5140Oe and  $M_s$  has 60.2emu/g and  $M_r$  has 33.5emu/g and if mineral is used as raw material, same properties are observed [23]. **In 2003**, Y.P.Fu prepared strontium hexaferrite powder by microwave- induced combustion process. The saturation magnetization of as-received product of strontium is 38emu/g and 525Oe intrinsic coercive force. After annealing for 2 hour at 1000°C, coercive force attains 1950Oe and saturation magnetization reaches 62emu/g [24]. **In 2004**, L.A.G.Cerda studied that strontium hexaferrite is prepared by sol-gel method. At 800°C pure phase formation is obtained from X-ray diffraction but alpha- $\text{Fe}_2\text{O}_3$  and gamma- $\text{Fe}_2\text{O}_3$  phase are formed when temperature is increased. The vibrating sample magnetometer was calculated  $M_s=56.97$  emu/g and  $H_c=4783$ Oe at 900°C calcined powder [25]. **In 2005**, A.Mali reported BaM nano- crystalline powder prepared by sol-gel auto combustion route using nitrate citrate gel. Oxides and nitrates homogenous mixture is formed after combustion. The results are not directly found from combustion process. They were found in two steps: monoferrite formation and between monoferrite and iron oxide formation at 900°C .The result was found that crystallite size greater than average grain size. But if calcinations temperature is increased, both sizes are increased. 1 hour calcined powder at 1000°C temperature best microstructure and magnetic result are found [26]. **In 2005**, J.Qiu. Showed that Cr- and Al-substituted BaM prepared by self- propagating combustion method with magnetic domain. The result shows that partially Al-substitution BaM improved microwave absorption property with high quality absorption microwave frequency 34.76DB but when Cr substitution exceeds 0.6, final product

is found of  $\text{CrCO}_3$ . In microwave band, first state of absorption energy of BaM is ferromagnetic resonance. Al-substituted BaM have ferromagnetic resonance frequency 14.56GHz and Cr-substitution decreases this frequency. The ferromagnetic resonance phenomenon of multi peak increases capacity of absorption in barium ferrite [27]. **In 2005**, J.Qiu reported that Al-substituted BaM synthesized by self-propagating combustion method. Al-substitution goes to lattice of barium hexaferrite shown by XRD pattern. The result shows that permittivity imaginary part move to huge frequency band and real part permittivity gradually increases with Al-substitution. At  $x=1.9$  Al-occupy  $4f_2$ ,  $4f_1$ ,  $12k$ ,  $2a$  site and 1.95GHz highest movement peak after  $12k$  occupy site. These occupations initially increase anisotropic field and then decrease [28]. **In 2005**, S.Sugimoto studied absorbing properties on BaM synthesized by modified co-precipitation route. In this, electromagnetic wave properties are examined with substitution of Co-Ti. The sintered sample at a  $T = 1423\text{K}$  for 5hrs with addition of  $\text{Bi}_2\text{O}_3$  in required weight. This enhanced property of high permeability = 25 and  $\mu_r = 10$  exists at 1 GHz. Slight matching thickness  $d_m = 3.1\text{mm}$  at 0.065GHz with fine microwave absorption property has been quite satisfied by shown sample. It's been observed that Ba has good applications to be a part of thinner microwave absorber in GHz [29]. **In 2005**, Y.P.Fu made strontium hexaferrite powders prepared by microwave-induced combustion process and discussed magnetic effect on Fe/Sr ratio. At  $1000^\circ\text{C}$  calcined powder of 11.6 Fe/Sr ratios for 2 hour, obtained 62emu/g saturation magnetization and 1950 Oe intrinsic coercive force. Without doped with metal element like Co-Ti etc, this process can obtain low coercivity of strontium powder [30]. **In 2006**, G.Xu reported BaM synthesized by sol-gel auto combustion. Citric acid was cheated with 11.5 molar ratios of  $\text{Fe}^{3+}$  and  $\text{Ba}^{2+}$  with different pH. The result was found at  $\text{pH}=10$ , well defined crystalline powder formed. At same pH value, intrinsic coercivity of 432KA/m is found and saturation magnetization is  $60\text{Am}^2/\text{kg}$  and remenance  $33\text{Am}^2/\text{Kg}$  with 1.5 molar ratio of citric acid to nitrate [31].

**In 2007**, N.J.Shirtcliffe studied highly Al-substituted BaM and SrM prepared by sol-gel auto-combustion method. This technique shows small particle size of ferrite powder. In this, half iron is replaced for aluminum in barium ferrite and strontium ferrite makes total substitution of iron with aluminum. Particles are obtained in materials less than 1 micrometer. When aluminum ferrite move from iron ferrite, morphological and structural changes are observed in material. Intermediate structure is observed with intermediate concentration with no dual phase [32]. **In 2007**, P.Shepherd reported that barium hexaferrite is synthesized by co-precipitation method. He investigated structural and magnetic properties of BaM. The result shows that in the frequency range of 1MHz to 1 GHz magnetic loss tangent and permeability measured

isothermally and isochronally was constant until 1300°C sintered temperature. At 1GHz 0.06 loss tangent, 1.3 relative permeability shows magnetic characteristics with high frequency. TGA observed 1050°C temperature range is suitable to obtain BaM. XRD pattern studied  $a = b = 5.895\text{Å}$ ,  $c = 23.199\text{Å}$ . In the range of 500MHz ferromagnetic characteristics are found with 452°C Curie temperature [33]. **In 2008**, A.Ataie studied BaM powder synthesized by sol-gel route. He has used inorganic agent as a starting raw material and studied characteristics of BaM. The results found that 12 molar ratio of Fe/Br is more significant. This initially was formed at 800°C but exactly at 1000°C. If molar ratio of Fe/Br increases from 10 to 12 then magnetic properties shows decrease in coercivity and increase in magnetization [34]. **In 2009**, F.M.M.Pereira studied M- type barium strontium hexaferrite prepared by ceramic route. He investigated dielectric and magnetic properties in the microwave frequency and radio frequency range. The result was agreed upon, if the frequency increases, the dielectric loss decreases and magnetic permittivity too increase. The BFO100 have permeability between 1.32-1.68 and SFO100 have 1.16 to 1.88 in frequency range 100MHz to 1.5GHz. The permittivity of SFO100 and BFO100 are 8.19 and 8.18 respectively at 1.5GHz but at 100MHz have 19.09 and 52.04 [35]. **In 2009**, H.R.Koohdar reported SrM nanocrystalline powder prepared by conventional route. He investigated particle size, morphology, phase composition with heat treatment and re-calcinations of hematite and carbonate at 1100°C. During heat treatment, the SrM was decomposed and hematite reduced to iron. SrM structure is much finer than it was initially after treatment. This was obtained at 850°C for 1 hour with 60cm<sup>3</sup>/gram gas flow. re- calcinations of SrM at 1000°C found finer structure than original. This effect increases with the coercivity [36]. **In 2009**, M.M.Hessien reported SrM via co- precipitation method. He has investigated magnetic properties with using of Egyptian celestite ore SrSO<sub>4</sub>. The well defined single phase formation was achieved at the 8.57 and 8 ratio of Fe<sup>3+</sup>/Sr<sup>2+</sup>. The crystallite size increased from 97.3 nm at 9.23 with molar ratios of Fe<sup>3+</sup>/Sr<sup>2+</sup> to 106.4nm at 8.57 ratios of Fe<sup>3+</sup>/Sr<sup>2+</sup>. For 8.57 ratio, 1000°C annealing temperature for 2 hours, high saturation magnetization was obtained and at different conditions wide coercivity produced [37]. **In 2010**, L.Junliang studied nano- powder of barium hexaferrite prepared by sol- gel auto combustion method with one step synthesis. They reported that fluffy particle with crystallite in 50-100nm diameter range obtained and each have single domain with less amount i.e. 260 Oe coercive field and 64.1emu/g saturation magnetization. EDTA and citric acid improve metal ion spatial distribution homogeneity and remove intermediate phase of poor and rich BaM. The sample support ceramic pad and on interior wall film strips developed temperature environment to BaM formation with microwave support in the time of gel auto combustion [38]. **In 2011**,

M.N.Ashiq reported Al-Cr substituted SrM nanomaterials prepared by co-precipitation method. The result shows that from EDX and XRD crystallite size in range 14-30 and from SEM 40-85nm range of crystallite size. The magnetic properties decrease as Al- Cr doping increases. The dielectric loss, dielectric constant, and a.c conductivity decreases with frequency. This shows that this doping material can be used in recording media due to high resistive material [39]. **In 2012**, K.Sadhana studied BaM of nanocrystalline and prepared by microwave hydrothermal method. The found out magnetic and structural properties of nanocrystalline powder. The results observed that average grain size of sintered sample lies from 185 to 490 nm. The sintered sample at 900°C for 1 hour obtained 1336Oe coercivity and 43emu/g saturation magnetization. The plate shaped shows hexaferrite at 950°C annealed [40]. **In 2012**, H.Luo reported highly Al- substituted strontium hexaferrite powder and it was synthesized via auto combustion method. The investigated magnetic properties and physical properties of hexagonal structure strontium ferrite. The result obtained at 1100°C for 12 hours in air heat treatment pure without secondary phase. Lattice parameter decreases with Al<sup>3+</sup> doping due to replacement of Fe<sup>3+</sup> by Al<sup>3+</sup>. EDX shows morphology change observed sphere to disk then rod. At x=4, coercivity increases but decreases after increasing doping value [41].

**In 2013**, C.J.Li reported nanofibres of BaM with Aluminum substitution. They have been synthesized by heat treatment for 2 hours at 1100°C calcinations temperature and electrospinning. The author has identified magnetic properties and magnetic structure. The results of BaFe<sub>12-x</sub>Al<sub>x</sub>O<sub>19</sub> reported that addition of Al<sup>3+</sup>, grain size decreases due to the replacement of Fe<sup>3+</sup> by Al<sup>3+</sup>. At x=0 hexagonal plate like structure is produced and x>0 rod like formed. At x=1 or less pure single phase is formed but greater case impurity were detected. The Al doping fuses into lattice of BaM. Magnetic properties show Al<sup>3+</sup> substitution coercivity increase 288.2 to 740.7 kA/m and saturation magnetization decreases from 63.92 to 29.70 Am<sup>2</sup>/kg [42]. **In 2014**, Y.Y.Meng researched ultrafine powder of BaM and it was prepared by sol-gel technique by using glycine gel as a raw material. The result shows that at 9/1 of Fe/Br single phase barium ferrite is formed. The structure of BaM is plate-like and crystallite size lies 55 to 110nm. At 900°C temperature with 12/9 molar ratio of glycine /nitrate obtained  $M_s$  67.7emu/g and  $H_c$  5750Oe [43]. **In 2014**, F.S.D.Jesus prepared SrM by high energy ball milling route. It was observed that structural transformation get promoted to SrM phase annealing treatment at temperature low i.e. 700°C. Saturation magnetization are over sensitive than the coercivity at annealing temperature between 700°C -1000°C. At 700°C annealing temperature, 5 hour milled powder, obtained maximum  $H_c=5.2$ kOe and  $M_s=60$  emu/g. No change is observed

in coercivity and saturation magnetization; if there is an increase in the annealing temperature but excess amount of hematite (second phase) decreases the saturation magnetization and increases the coercivity from 5.2 to 6.6kOe [44]. **In 2014**, M.G.Hasab prepared SrM using sol gel auto combustion technique. It was calcined the burned powder of SrM at different temperature range i.e. 700 to 900°C to make a single phase. It has been achieved nano size particle and single phase of SrM at 800°C temperature and also found coercivity 6238Oe and crystallite size of SrM is 27nm [45]. **In 2015**, A.H.Najafabadi reported Al-substituted BaM by sol gel auto combustion technique. This result shows that initially coercivity increases with Al-substituted but at higher extent it was decreased and saturation magnetization was increased with increased value of doped cation. It was explained based on of magnetocrystalline anisotropy and decreases particle size [46]. **In 2015**, S.M.Mirkazemi analyzed nano-sized strontium hexaferrite powder prepared by sol-gel auto combustion method CTAB (cetyltrimethylammonium bromide) surfactant. Magnetic properties and microstructure used were studied. The addition of CTAB (cetyltrimethylammonium bromide) results show reduces Fe<sub>2</sub>O<sub>3</sub> residual amount and increases coercivity value from 4950.89 to 5221.47Oe and saturation magnetization 48.41 to 60.40 at 800°C temperature. If without CTAB calcinations temperature increases, intrinsic coercivity also increases and maximum magnetization but if both increases, intrinsic coercivity diminish [47]. **In 2015**, V.G.Kostishyn observed Multiferroics properties of M- type strontium hexaferrite. Hexagonal ferrite ceramic synthesized by modified technology by adding boron oxide. During sintering with addition O<sub>2</sub>. It possesses Multiferroics properties at room temperature and more closer than other Multiferroics like BiFeO<sub>3</sub>. 45μC/cm<sup>2</sup> electronic polarization, 25mV/Oe magnetometer and greater than 4% magnetoelectric ratio enhanced by fabricated sample. In substituted ferrite, 9-10% value of magnetization helps to make magnetoelectric device. Here, magnetoelectric effect and spontaneous electronic polarization is advanced with some required demonstration [48]. **In 2015**, J.Liu reported nano- powder of barium hexaferrite surface carbonized layers and it was found out Tunable microwave absorbing properties. The amorphous carbon having thickness 10–30nm range consists on carbonized layer. The carbonized layer on ferrite improves dielectric loss and interfacial. Increase the layer, obtained fine property of microwave absorbing and impedance matching. This result provide multiphase of absorbing electromagnetic wave with more desirable performance [49]. **In 2015**, T.Li observed solution of M-type hexagonal structure SrM using egg- white. Magnetic and structural properties were analyzed. It was found that 1000-1300°C sintering temperature and 1:8 of Sr/Fe, pure phase is observed. If add Egg white which is binder also effect on magnetic property and crystallinity. It

is perfectly obtained at 1200°C sintering temperature, 3g egg-white binder and 1:8 of Sr/Fe [50]. **In 2016**, F.Rhein studied Al<sup>3+</sup> substituted SrM with enhancement of saturation magnetization and coercivity. The result shows that above 1100°C Calcinations temperature pure phase formed if Fe<sup>3+</sup> substituted by Al<sup>3+</sup>, prevents particle growth and increase coercivity above 1000°C calcinations temperature but milling process magnetic properties decreases specially x=0,1. The small crystallite higher order Al<sup>3+</sup> strontium ferrite formed when annealing 1000°C in NaCl. Coercivity and saturation magnetization simultaneously improve by annealing and milling process rather than solid state reaction [51]. **In 2016**, P.Sivakumar reported magnetic properties of nanoparticles of strontium hexaferrite with facile sonochemical preparation. The sample prepared by facile strategy shows crystallite size 44nm and  $a = 0.5884$  and  $c = 23.035$ . The diameter range lies 50–500nm at low magnification. The EDX shows 1:12 of strontium to iron. The TGA observed 462°C Curie temperature. The super conducting quantum interference device shows magnetic property in temperature range 4 to 300K which found less reliable magnetization than bulk strontium ferrite [52]. **In 2016**, S.Torkin prepared Al- substituted SrM with route of sol gel auto combustion. To make a SrFe<sub>1-x</sub>Al<sub>x</sub>O<sub>19</sub> (1 <= 4) nanocrystalline synthesis heat treatment in auto combustion doping in air. The result found that Fe<sub>2</sub>O<sub>3</sub> secondary phase exists when at 900°C temperature sample was calcined. At 1200°C calcinations temperature, pure strontium hexaferrite is formed and  $H_c = 5.1\text{kOe}$  and  $M_r = 33\text{emu/g}$  and  $M_s = 59.7\text{emu/g}$  obtained but aluminum doping concentration increases then magnetic saturation gradually decreases and initially coercivity decreases and further increases. At x = 2 alumina doping  $H_c = 9.1\text{kOe}$  is obtained than pure strontium hexaferrite coercivity i.e. 7.5kOe [15].

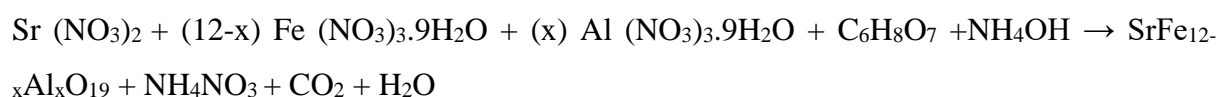
## CHAPTER-3

### EXPERIMENTAL DETAIL

---

#### 3.1 Sample Preparation

To prepared  $\text{SrFe}_{12-x}\text{Al}_x\text{O}_{19}$  ( $x= 0.0, 1.0, 2.0$ ), strontium nitrate ( $\text{Sr}(\text{NO}_3)_2$ ), iron nitrate  $\text{Fe}((\text{NO}_3)_3 \cdot 9\text{H}_2\text{O})$ , aluminum nitrate ( $\text{Al}(\text{NO}_3)_3 \cdot 9\text{H}_2\text{O}$ ), citric acid ( $\text{C}_6\text{H}_8\text{O}_7$ ) with 99% purity are used. The sample composition was taken by the following reaction equation



The equimolar amount of strontium nitrate, iron nitrate, citric acid, and alumina nitrate dissolved in 200ml de-ionized water and stirred for 15 hours with constant stirring rate. To maintain pH 7 a small amount of ammonia were slowly added in the nitrate solution during stirring. After homogenous mixing, the solution were stirring at  $70^\circ\text{C}$  temperature till the auto combustion a Finally brown color precursor was formed and allowed it to cool till room temperature. The as prepared powders were grounded by pestle and mortar for 30 minutes. Further the powder was calcined in muffle furnace at  $150^\circ\text{C}$  in ambient atmosphere for 3 hours. In similar way the Al-substituted BaM were prepared, where barium nitrate were used instead of strontium nitrate.

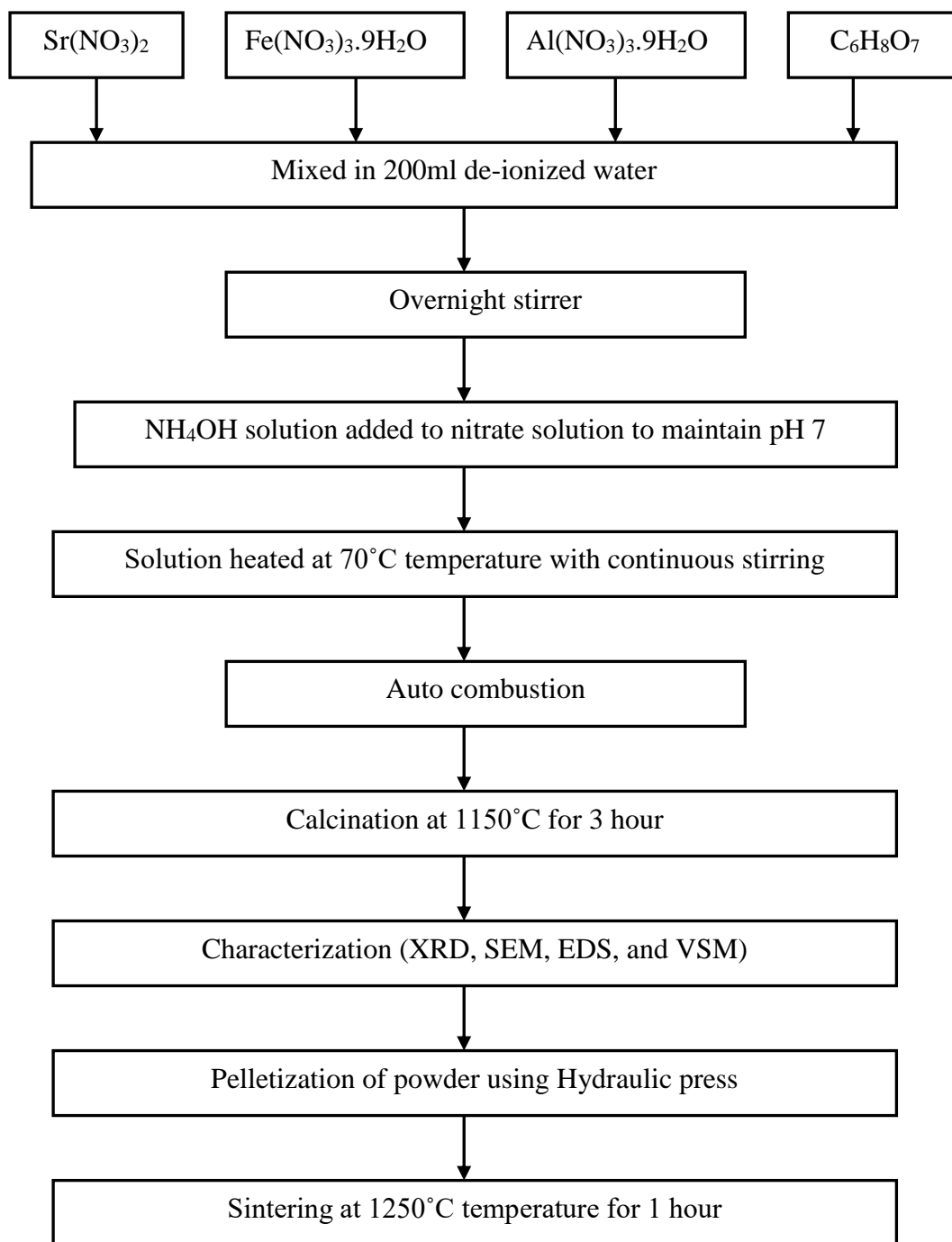


**Fig.3.1** Flow chart for preparation of Al-substituted SrM

## CHAPTER-4

### RESULT AND DISCUSSION

---

#### 4.1 X-Ray Diffraction

X-Ray diffraction patterns of Al- substituted BaM and SrM calcined at 1150°C are shown in fig.4.1. The single phase BaM and SrM were obtained and in agreement with JCPDS card no. 00-0070276 and 01-0720739. A slight shifts to higher 2 theta were obtained in Al-substituted powders due to strain induced by Al<sup>3+</sup> ion with smaller ionic radii (0.0675Å).

The lattice parameter 'a' and 'c' were calculated by this formula [53],

$$\frac{1}{d^2} = \frac{4}{3} \left( \frac{h^2+hk+k^2}{a^2} \right) + \frac{l^2}{c^2} \quad (1)$$

Where  $h, k, l$  are miller indices and  $d$  is interplanar spacing. Volume ( $V$ ) of the unit cell were calculate by [61]

$$V = \cos 30^\circ a^2 c \text{ (}\text{Å}^3\text{)} \quad (2)$$

The crystallite size ( $D$ ) of SrM and BaM were calculated by Debye Scherrer formula [54]:

$$D = \frac{k\lambda}{\beta \cos \theta} \text{ (nm)} \quad (3)$$

Where  $\beta$  indicate FWHM (radian),  $K$  is Scherrer constant (0.94 for hexagonal structure),  $\lambda$  depicts X-ray wavelength (1.54Å) and  $\theta$  describe angle.

X-ray density is calculated by:

$$\rho_{\text{(x-ray)}} = \frac{ZM}{N_A V} \left( \frac{g}{\text{cm}^3} \right) \quad (4)$$

Where,  $Z$  is the number of molecules per unit cell (In BaM unit cell consist of two formula unit or two molecules structure hence,  $Z = 2$ ),  $M$  is the molecular weight,  $N_A$  Avogadro's number,  $V$  is volume of unit cell [54].

Green and Sintered density of the pellets were calculated by [55]

$$\rho = \frac{\text{mass}}{\text{volume}} \left( \frac{g}{\text{cm}^3} \right) \quad (5)$$

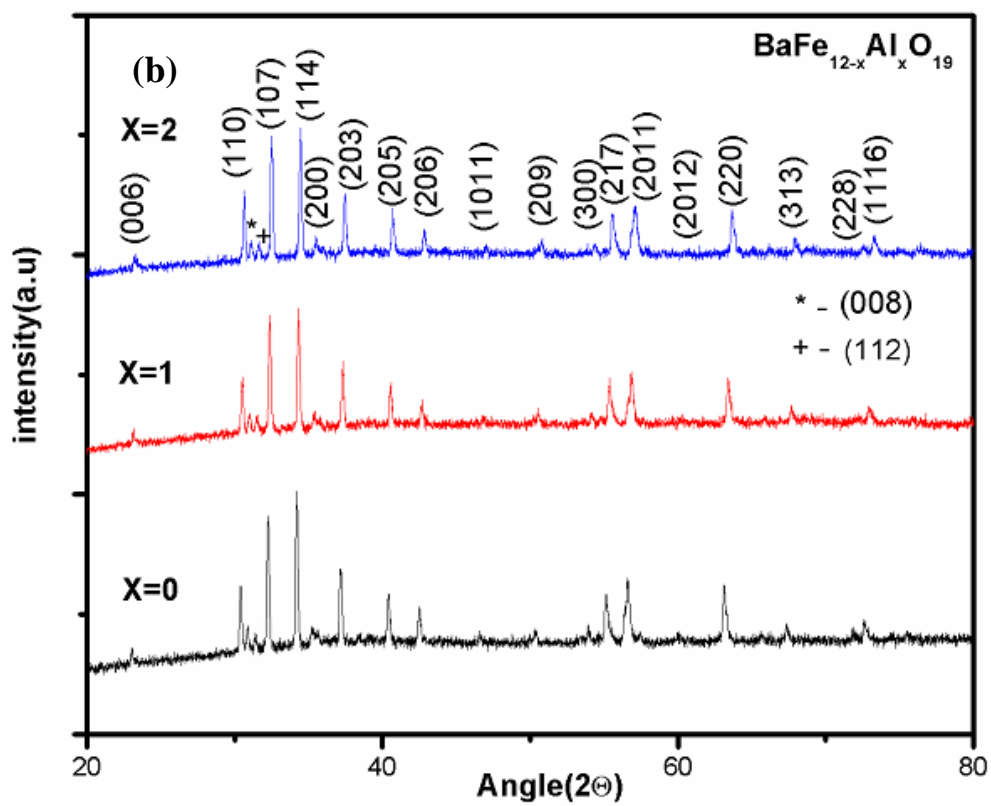
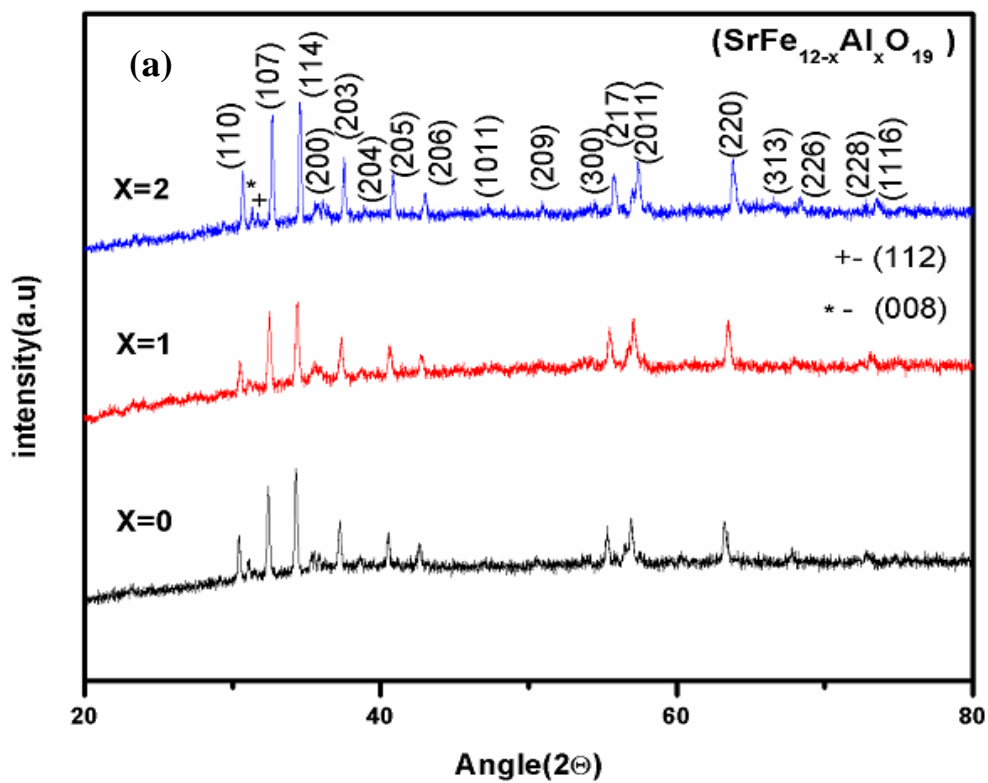


Fig.4.1 XRD patterns for (a)  $\text{SrFe}_{12-x}\text{Al}_x\text{O}_{19}$ , (b)  $\text{BaFe}_{12-x}\text{Al}_x\text{O}_{19}$

**Table 4.1** Calculated structural parameters of Al-substituted BaM and SrM

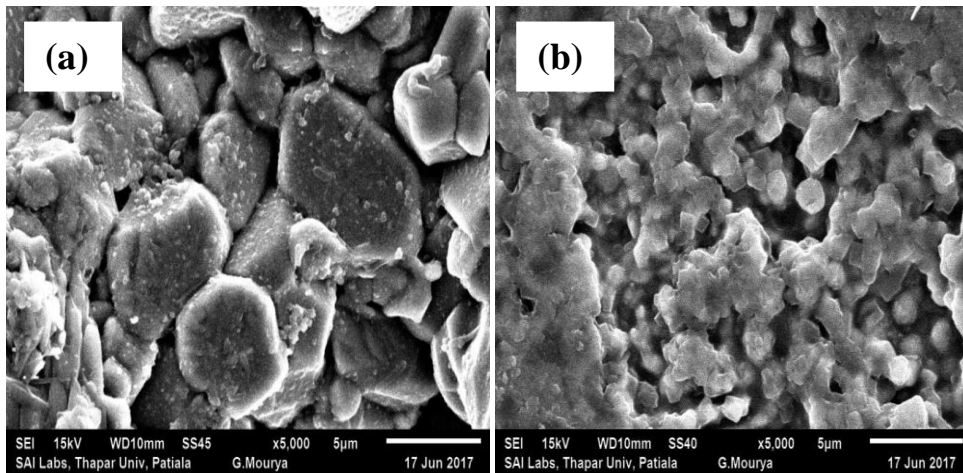
	a(A°)	c(A°)	V(A° <sup>3</sup> )	C.S(nm)	$\rho$ (g/cc)	$\rho_{\text{sinter}}$ (g/cc)	Porosity (%)
<b>BaFe<sub>12</sub>O<sub>19</sub></b>	5.89	23.19	696.25	66.59	5.30	4.45	16.05
<b>BaFe<sub>11</sub>AlO<sub>19</sub></b>	5.87	23.13	689.30	61.46	5.22	4.04	22.53
<b>BaFe<sub>10</sub>Al<sub>2</sub>O<sub>19</sub></b>	5.83	22.99	678.87	72.53	5.15	3.55	31.05
<b>SrFe<sub>12</sub>O<sub>19</sub></b>	5.88	23.05	690.16	72.21	5.11	4.55	10.91
<b>SrFe<sub>11</sub>AlO<sub>19</sub></b>	5.87	22.96	684.79	54.16	5.01	3.75	25.13
<b>SrFe<sub>10</sub>Al<sub>2</sub>O<sub>19</sub></b>	5.85	22.90	678.62	57.82	4.92	3.26	33.76

#### 4.2 Scanning Electron Microscopy (SEM)

Fig. 4.2 shows the representative SEM micrographs of fractured surface of pure and Al-substituted sintered SrM. The micrograph shows that Al substitution reduces the particle size. It is clear from the Fig 4.2 that particle size was reduced from  $\sim 4.5 \mu\text{m}$  for pure SrM to  $1.8 \mu\text{m}$  Al ( $x = 2.0$ ) substituted strontium hexaferrite. Crystallinity index ( $I_{\text{cry}}$ ) were calculated from following relation:

$$I_{\text{cry}} = \frac{D_p(\text{SEM,TEM})}{\tau(\text{XRD})} \quad (7)$$

Where  $D_p$  is average particle size obtained from micrograph and  $\tau$  is average crystallite size as obtained from Scherer equation. The calculated values shown in table 4.2. The calculated values show drastic reduction  $I_{\text{cry}}$ , this suggests that reduction in the particle size is mainly by Al-substitution. There might be possibility that a small fraction of  $\text{Al}_2\text{O}_3$  remained unsubstituted which cause pinning effect and inhibit the particle growth.

**Fig.4.2** SEM image of sintered fractured pellets of  $\text{SrFe}_{12-x}\text{Al}_x\text{O}_{19}$  (a)  $x = 0$ , (b)  $x = 2$

**Table 4.2** Variation of particle size with Al substitution

Sample	Particle size( $\mu\text{m}$ )	I <sub>Crystal</sub> (A.U)
SrFe <sub>12</sub> O <sub>19</sub>	4.46	61.82
SrFe <sub>10</sub> Al <sub>2</sub> O <sub>19</sub>	1.77	30.56

### 4.3 Energy Dispersive Spectroscopy (EDS)

The EDS spectrums of synthesized powders are shown in fig.4.3. The peaks in EDS at different energy level depict the presence of different elements. The EDS spectrum illustrates the elemental composition of as synthesized materials which confirm the presence of Sr, O and Fe. In the substituted sample, a peak of Al is also present. The atomic and weight % shown in table 4.3

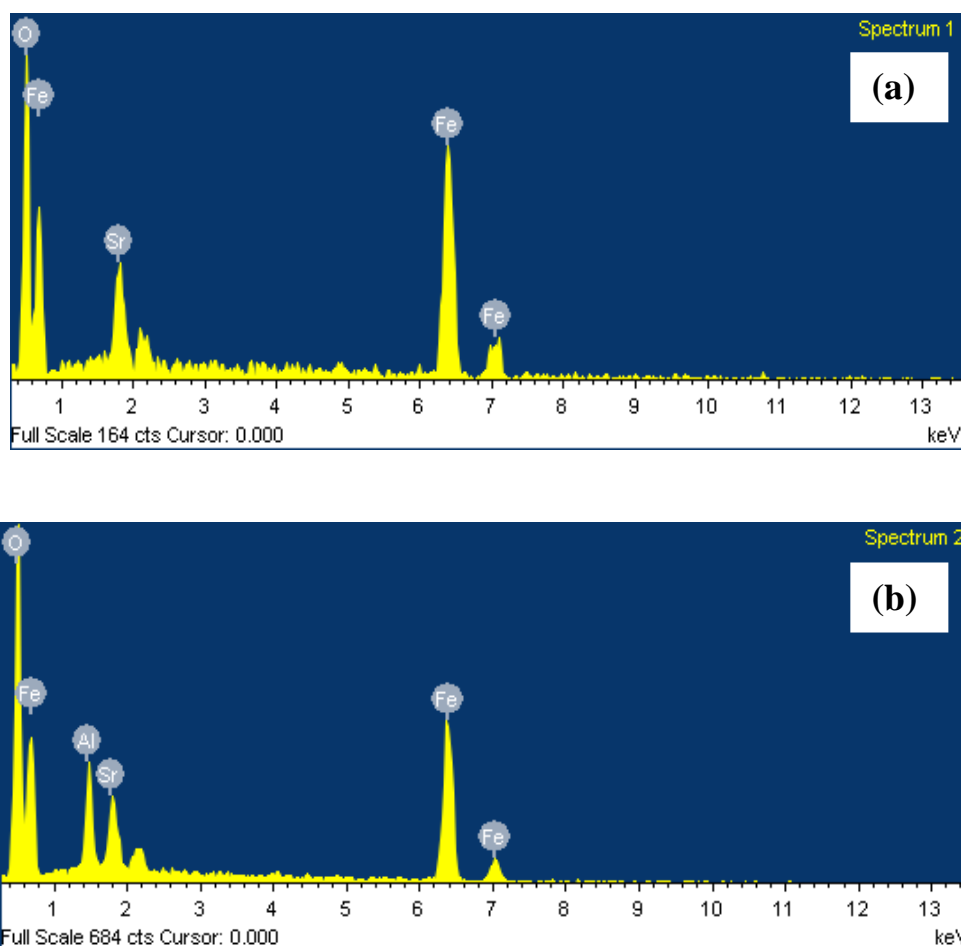


**Fig 4.3** EDS Spectrum of sintered fractured pellet SrFe<sub>12-x</sub>Al<sub>x</sub>O<sub>19</sub> (a) x=0 (b) x=2

**Table 4.3** Element analysis for SrFe<sub>12</sub>O<sub>19</sub> and SrFe<sub>10</sub>Al<sub>2</sub>O<sub>19</sub>

Element	Weight%	Atomic%	Weight%	Atomic%
	SrFe <sub>12</sub> O <sub>19</sub>		SrFe <sub>10</sub> Al <sub>2</sub> O <sub>19</sub>	
<b>O K</b>	25.48	55.53	32.54	61.64
<b>Fe K</b>	65.42	40.85	53.06	28.79
<b>Sr L</b>	9.10	3.62	8.51	2.94
<b>Al K</b>	-	-	5.90	6.62
<b>Total</b>	100		100	

### 4.3 Magnetic properties

Magnetic properties of powder and sintered pellets are studied by vibrating sample magnetometer upto a maximum field of 1.0 T and 1.5 T. Fig. 4.5 shows the M-H loop of pure and Al-substituted SrM and BaM. It is observed that saturation magnetization decreases and coercivity increases with Al substitution. Further, Al-substituted powder shows non saturating behavior at 1T field. For sintered pellets, similar trend is observed i.e. the saturation magnetization decreases and coercivity increases with Al substitution. However, for pure samples coercivity of sintered pellets is found to be less as compared to powder. This is due the large grain size in sintered pellet. However, very high coercivity i.e. max upto 10kOe (x=2) is observed in sintered pellets. The decrease in saturation magnetization may be due to the Al<sup>3+</sup> (0  $\mu_B$ ) ions substituting Fe<sup>3+</sup> (5  $\mu_B$ ) at spin up sites in the hexagonal crystal structure. The drastic increase in coercivity might be attributed to lattice shrinkage and the pinning action by unsubstituted Al<sub>2</sub>O<sub>3</sub>, which provide hindrance to particle growth and demagnetization [56]. Residual magnetism ( $M_r$ ) was measured directly from hysteresis loop in both cases. Further, squareness ratio SQR is calculated by using  $M_r/M_s$  the values are fundamentally a measure of squareness of the hysteresis loop. SQR plays an important role in permanent magnets and recording media application [33]. Table 4.4 and 4.5 shows the magnetic properties of BaM/SrM powders and pellets respectively.

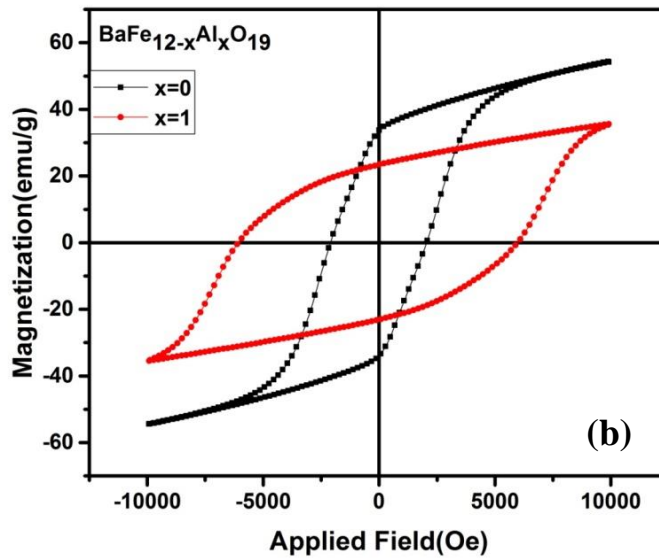
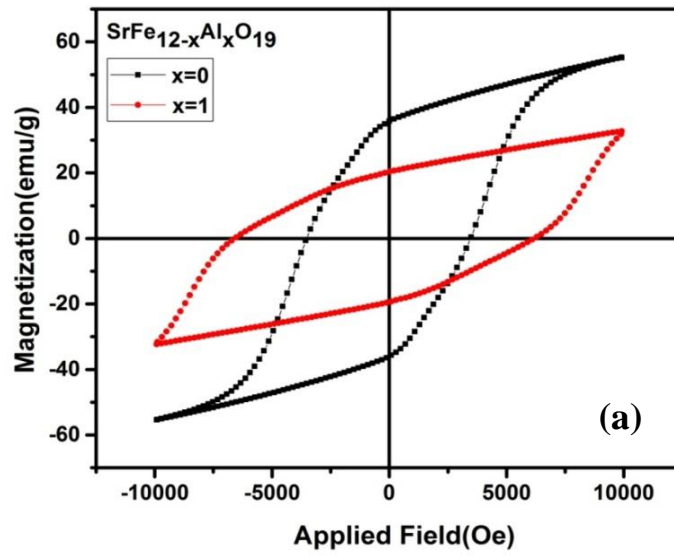


**Fig.4.4** Magnetization curve of (a)  $\text{SrFe}_{12-x}\text{Al}_x\text{O}_{19}$  (b)  $\text{BaFe}_{12-x}\text{Al}_x\text{O}_{19}$

**Table 4.4** Magnetic properties of Al-substituted BaM and SrM powder

Sample	$M_r$ (emu/g)	$M_s$ (emu/g)	$M_r/M_s$	$H_c$ (kOe)
$\text{BaFe}_{12}\text{O}_{19}$	33.36	54.35	0.61	2.07
$\text{BaFe}_{11}\text{AlO}_{19}$	23.27	35.55	0.65	6.01
$\text{SrFe}_{12}\text{O}_{19}$	35.90	55.29	0.65	3.49
$\text{SrFe}_{11}\text{AlO}_{19}$	19.89	32.50	0.61	6.39

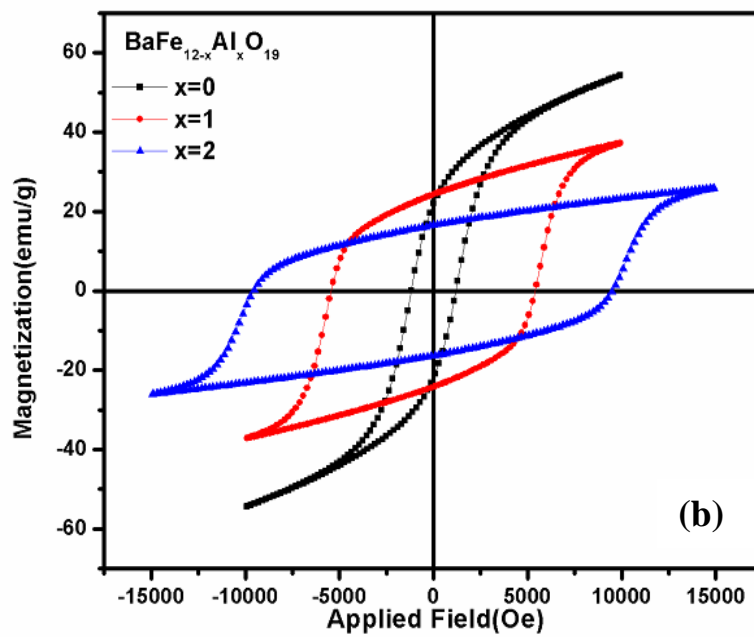
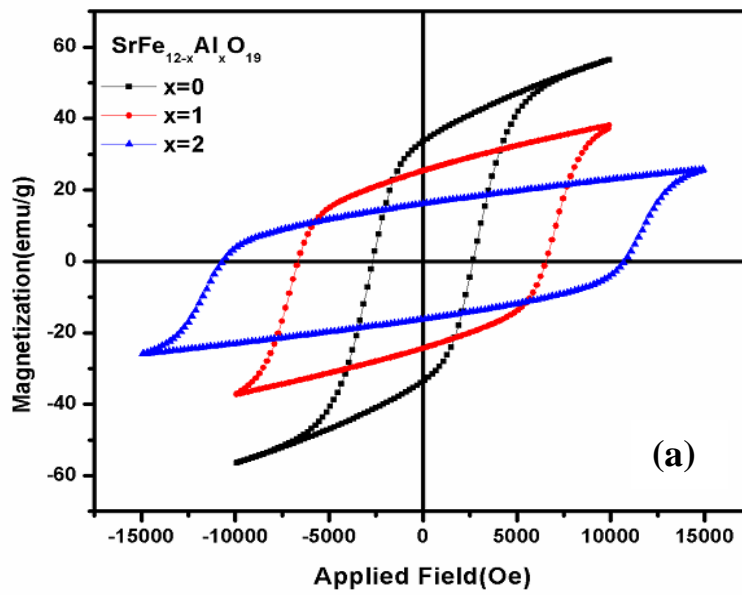


**Fig.4.5**  $M$ - $H$  behavior of sintered fractured pellet (a)  $\text{SrFe}_{12-x}\text{Al}_x\text{O}_{19}$  (b)  $\text{BaFe}_{12-x}\text{Al}_x\text{O}_{19}$

**Table 4.5** *M-H* Behaviour of sintered fractured pellet of Al-substituted SrM and BaM

<b>Sample</b>	<b><math>M_r</math>(emu/g)</b>	<b><math>M_s</math>(emu/g)</b>	<b><math>M_r/M_s</math></b>	<b><math>H_c</math>(kOe)</b>
<b>BaFe<sub>12</sub>O<sub>19</sub></b>	21.90	54.32	0.40	1.19
<b>BaFe<sub>11</sub>AlO<sub>19</sub></b>	24.27	37.23	0.65	5.41
<b>BaFe<sub>10</sub>Al<sub>2</sub>O<sub>19</sub></b> ( $\pm 1.5$ T)	16.44	26.00	0.63	9.58
<b>SrFe<sub>12</sub>O<sub>19</sub></b>	11.68	52.52	0.22	2.67
<b>SrFe<sub>11</sub>AlO<sub>19</sub></b>	24.86	37.64	0.66	6.60
<b>SrFe<sub>10</sub>Al<sub>2</sub>O<sub>19</sub></b> ( $\pm 1.5$ T)	16.13	25.85	0.62	10.70

## **CHAPTER-5**

### **CONCLUSION AND FUTURE SCOPE**

---

#### **Conclusion**

Aluminium substitution barium and strontium M-type hexaferrite (BaM and SrM) were synthesized by sol-gel auto combustion method. The XRD confirms that barium and strontium hexaferrite have hexagonal structure and single phase. The crystallite size is reduced due to less ionic radius of aluminium. Lattice constant also found to decrease with substitution. Particle size is determined by scanning electron microscopy and it lies in the range of 4.46-1.76 $\mu$ m. EDS shows that all the required elements are present in the samples. The magnetic properties of Al-substituted BaM and SrM powders and sintered pellets are determined by vibrating sample magnetometer, which shows that coercivity increases as the aluminium substitution increases. Squareness ratio lies in the range 0.40-0.63 for aluminium substitution barium hexaferrite and 0.22-0.62 for aluminium substitution strontium hexaferrite.

#### **Future Scope**

The future scope of the thesis will focus on application of such ferrites for high frequency range above (50GHz).

## REFERENCES

---

- [1] M.Sugimoto, "The past, present, and future of ferrites," *Journal of the American Ceramic Society*, vol. **82**, no.2, pp.269-280 (1999).
- [2] J.A.Kohn, D.W.Eckart, and C.F.Cook, "Crystallography of the hexagonal ferrites," *Science*, vol.**172**, no.3983, pp.519-525 (1971).
- [3] M.N.Ashiq, M.J.Iqbal, and I.H.Gul, "Effect of Al–Cr doping on the structural, magnetic and dielectric properties of strontium hexaferrite nanomaterials," *Journal of Magnetism and magnetic materials*, vol. **323**, no.3, pp.259-263 (2011).
- [4] M.B.Amin, and J.R.James, "Techniques for utilization of hexagonal ferrites in radar absorbers. Part 1: Broadband planar coatings," *Radio and Electronic Engineer*, vol.**51**, no.5, pp.209-218(1981).
- [5] R.C.Pullar, "Hexagonal ferrites: a review of the synthesis, properties and applications of hexaferrite ceramics," *Progress in Materials Science*, vol. **57**, no.7, pp.1191-1334 (2012).
- [6] P.Eugene, et al., *Chem. Sustain. Dev*, vol.**10**, pp.161 (2002).
- [7] Z.Li, and F.Gao, "Chemical bond and hardness of M-, W-type hexagonal barium ferrites," *Canadian Journal of Chemistry*, vol. **89**, no.5, pp.573-576(2011).
- [8] J.Smit, and H.P.J.Wijn, "Ferrites: physical properties of ferrimagnetic oxides in relation to their technical applications," *Phillips Technical Library, Eindhoven, the Netherland* (1959).
- [9] M.A.Ahmed, N.Okasha, and R.M.Kershi, "Influence of rare-earth ions on the structure and magnetic properties of barium W-type hexaferrite," *Journal of Magnetism and Magnetic Materials*, vol.**320**, no.6, pp.1146-1150 (2008).
- [10] B.X.Gu, "Magnetic properties of X-type  $Ba_2Me_2Fe_{28}O_{46}$  (Me= Fe, Co, and Mn) hexagonal ferrites," *Journal of applied physics*, vol. **71**, no.10, pp. 5103-5106 (1992).
- [11] G.Albanese, A.Deriu, F.Licci, and S.Rinaldi, "Preparation and magnetic characterization of the  $Ba_2Zn_{2-2x}Cu_{2x}Fe_{12}O_{22}$  hexagonal ferrites," *IEEE Transactions on Magnetics*, vol.**14**, no.5, pp. 710- 712 (1978).
- [12] O.Kimura, M.Matsumoto, and M.Sakakura, "Magnetic properties of Sr substituted  $Co_2Z$  magnetoplumbite for ultra high frequency uses," *Journal of the Japan Society of Powder and Powder Metallurgy*, vol. **42**, no.1, pp. 27 -33(1995).

- [13] R.C.Pullar, and A.K.Bhattacharya, "The synthesis and characterization of  $\text{Co}_2\text{X}$  ( $\text{Ba}_2\text{Co}_2\text{Fe}_{28}\text{O}_{46}$ ) and  $\text{Co}_2\text{U}$  ( $\text{Ba}_4\text{Co}_2\text{Fe}_{36}\text{O}_{60}$ ) ferrite fibres, manufactured from a sol-gel process," *Journal of materials science*, vol. **36**, no.19, pp. 4805 -4812(2001).
- [14] P.B.Braun, "The crystal structures of a new group of ferromagnetic compound", *Philos Res Rep*, vol.**12**, pp. 491(1957).
- [15] S.Torkian, A.Ghasemi, R.ShojaRazavi, and M.Tavoosi, "Structural and Magnetic Properties of High Coercive Al-Substituted Strontium Hexaferrite Nanoparticles," *Journal of Superconductivity & Novel Magnetism*, vol.**29**, no.6, pp. 1627-1640(2016).
- [16] G.A.Jones, S.F.H.Parker, J.G.Booth, and D.Simkin, "Domain structure of the single crystal hexagonal ferrite,  $\text{Co}/\text{sub } 2/\text{X}$ ," *IEEE Transactions on Magnetics*, vol.**26**, no. 5, pp.2804-2806 (1990).
- [17] A.Verma, O.P.Pandey, and P.Sharma, "Strontium ferrite permanent magnet- an overview," *Indian journal of engineering & Material Science*, vol. **7**, pp. 364- 369(2000).
- [18] M.Chen, and D.E. Nikles, "Synthesis, Self-Assembly, and Magnetic Properties of  $\text{Fe}_x\text{Co}_y\text{Pt}_{100-x-y}$  Nanoparticles," *Nano Letters*, vol.**2**, no.3, pp.211-214 (2002.).
- [19] L.L.Hench, and J.K.West, "The sol-gel process," *Chemical reviews*, vol.**90**, no.1, pp.33-72 (1990).
- [20] L.Li, K.Chen, H.Liu, G.Tong, H.Qian, and B.Hao, "Attractive microwave-absorbing properties of M-Ba $\text{Fe}_{12}\text{O}_{19}$  ferrite," *Journal of Alloys and Compounds*, vol.**557**, pp.11-17(2013).
- [21] J.Huo, L.Wang, and H.Yu, "Polymeric nanocomposites for -electromagnetic wave absorption," *Journal of materials science* vol.44, no.15, pp.3917-3927(2009).
- [22] C.Sürig, K.A.Hempel, and D.Bonnenberg, "Formation and microwave absorption of barium and strontium ferrite prepared by sol-gel technique," *Applied physics letters*, vol. **63**, no.20, pp. 2836-2838 (1993).
- [23] Z.B.Guo, W.Ding, W.Zhong, J.R.Zhang, and Y.W.Du. "Preparation and magnetic properties of  $\text{SrFe}_{12}\text{O}_{19}$  particles prepared by the salt-melt method," *Journal of magnetism and magnetic materials*, vol.**175**, no.3, pp.333-336 (1997).
- [24] Y.P.Fu, C.H.Lin, and K.Y.Pan, "Strontium hexaferrite powders prepared by a microwave-induced combustion process and some of their properties," *Journal of alloys and compounds*, vol.**349**, no.1, pp. 228- 231 (2003).

- [25] L.A.García, and P.J.Reséndiz-Hernández, "Study of SrFe<sub>12</sub>O<sub>19</sub> synthesized by the sol–gel method," *Journal of alloys and compounds*, vol. **369**, no.1, pp.182-184 (2004).
- [26] A.Mali, and A.Ataie, "Structural characterization of nano-crystalline BaFe<sub>12</sub>O<sub>19</sub> powders synthesized by sol–gel combustion route," *Scripta Materialia*, vol. **53**, no.9, pp. 1065-1070(2005).
- [27] J.Qiu, M.Gu, and H.Shen, "Microwave absorption properties of Al-and Cr-substituted M-type barium hexaferrite," *Journal of Magnetism and Magnetic Materials*, vol.**295**, no.3, 263-268(2005).
- [28] J.Qiu, Q.Zhang, M.Gu, and H.Shen, "Effect of aluminum substitution on microwave absorption properties of barium hexaferrite," *Journal of applied physics*, vol. **98**, no.10, pp.103905 (2005).
- [29] S.Sugimoto, K.Haga, T.Kagotani, and K.Inomata, "Microwave absorption properties of Ba M-type ferrite prepared by a modified co precipitation method," *Journal of magnetism and magnetic materials*, vol. **290**, pp. 1188-1191(2005).
- [30] Y.P.Fu, and C.H.Lin, "Fe/Sr ratio effect on magnetic properties of strontium ferrite powders synthesized by microwave-induced combustion process," *Journal of Alloys and Compounds*, vol. **386**, no.1 pp. 222-227 (2005).
- [31] G.Xu, G.Xu, H.Ma, M.Zhong, J.Zhou, Y.Yue, and Z.He, "Influence of pH on characteristics of BaFe<sub>12</sub>O<sub>19</sub> powder prepared by sol–gel auto-combustion," *Journal of Magnetism and Magnetic Materials*, vol. **301**, no.2, pp. 383-388(2006).
- [32] J.Shirtcliffe Neil, S.Thompson, E.S.O.Keefe, S.Appleton, and C.C.Perry, "Highly aluminium doped barium and strontium ferrite nanoparticles prepared by citrate auto-combustion synthesis," *Materials research bulletin*, vol. **42**, no.2, pp. 281-287(2007).
- [33] P.Shepherd, K.K.Mallick, and R.J.Green, "Magnetic and structural properties of M-type barium hexaferrite prepared by co-precipitation," *Journal of magnetism and magnetic materials*, vol. **311**, no.2 pp. 683-692(2007).
- [34] A.Ataie, and A.Mali, "Characteristics of barium hexaferrite nanocrystalline powders prepared by a sol-gel combustion method using inorganic agent," *Journal of Electroceramics*, vol.**21**, no.1, pp. 357-360(2008).
- [35] F.M.M.Pereira, M.R.P.Santos, R.S.T.M.Sohn, J.S.Almeida, A.M.L. Medeiros, M.M. Costa, and A.S.B.Sombra, "Magnetic and dielectric properties of the M-type barium strontium hexaferrite (Ba<sub>x</sub>Sr<sub>1-x</sub>Fe<sub>12</sub>O<sub>19</sub>) in the RF and microwave (MW) frequency range," *Journal of Materials Science: Materials in Electronics*, vol. **20**, no.5, pp.408- 417 (2009).

- [36] H.R.Koohdar, S.A.S.Ebrahimi, A.Yourdkhani, R.Deaghan, and F.Zajkaniha, "Optimization of hydrogen dynamic heat treatment and re-calcination for preparation of strontium hexaferrite nanocrystalline powder," *Journal of Alloys and Compounds*, vol. **479**, no.1, pp. 638-641 (2009).
- [37] M.M.Hessien, M.M.Rashad, M.S.Hassan, and K.E.Barawy, "Synthesis and magnetic properties of strontium hexaferrite from celestite ore," *Journal of Alloys and Compounds*, vol. **476**, no.1, pp. 373-378 (2009).
- [38] L.Junliang, Z.Yanwei, G.Cuijing, Z.Wei, and Y.Xiaowei, "One-step synthesis of barium hexaferrite nano-powders via microwave-assisted sol-gel auto-combustion," *Journal of the European Ceramic society*, vol.**30**, no.4, pp.993-997(2010).
- [39] M.N.Ashiq, M.J.Iqbal, and I.H.Gul, "Effect of Al-Cr doping on the structural, magnetic and dielectric properties of strontium hexaferrite nanomaterials," *Journal of Magnetism and magnetic materials*, vol. **323**, no.3, pp. 259-263(2011).
- [40] K.Sadhana, K.Praveena, S.Matteppanavar, and B.Angadi, "Structural and magnetic properties of nanocrystalline BaFe<sub>12</sub>O<sub>19</sub> synthesized by microwave-hydrothermal method," *Applied Nanoscience*, Vol., **2**, pp.1-6(2012).
- [41] H.Luo, B.K.Rai, S.R.Mishra, V.V.Nguyen, and Liu, J.P.Liu, "Physical and magnetic properties of highly aluminum doped strontium ferrite nanoparticles prepared by auto-combustion route," *Journal of Magnetism and Magnetic Materials*, vol. **324**, no.17, pp. 2602-2608(2012).
- [42] C.J.Li, B.N.Huang, and J.N.Wang, "Effect of aluminum substitution on microstructure and magnetic properties of electrospun BaFe<sub>12</sub>O<sub>19</sub> nanofibers," *Journal of Materials Science*, vol. **48**, pp. 1-9(2012).
- [43] Y.Y.Meng, M.H.He, Q.Zeng, D.L.Jiao, S.Shukla, R.V.Ramanujan, and Z.W.Liu, "Synthesis of barium ferrite ultrafine powders by a sol-gel combustion method using glycine gels," *Journal of alloys and compounds*, vol. **583**, pp. 220-225(2014).
- [44] F.S.D.Jesús, A.M.B.Miró, R.V.Claudia Alicia Cortes-Escobedo, and S. Ammar, "Mechanosynthesis, crystal structure and magnetic characterization of M-type SrFe<sub>12</sub>O<sub>19</sub>," *Ceramics International*, vol. **40**, no.3, pp. 4033-4038(2014).
- [45] M.G.Hasab, and Z.Shariati, "Magnetic properties of Sr-Ferrite Nano-Powder synthesized by Sol-Gel auto combustion method," *International Journal of Chemical, Nuclear, Metallurgical and Materials Engineering*, vol. **8**, no.10, pp. 10(2014).
- [46] A.H.Najafabadi, R.Mozaffarinia, and A.Ghasemi, "Microstructural Characteristics and Magnetic Properties of Al- Substituted barium Hexaferrite Nanoparticles Synthesized by

- Auto- Combustion sol- Gel Processing,” *J Supercond Nov Magn.* vol. **28**, pp. 2821-2830(2015).
- [47] S.M.Mirkazemi, S.Alamolhoda & Z.Ghiami, “Erratum to: Microstructure and Magnetic properties of SrFe<sub>12</sub>O<sub>19</sub> Nano- Sized Powders Prepared by Auto -Combustion method with CTAB Surfactant,” *J supercond Nov Magn.* vol. **28**, pp. 1551- 1558 (2015).
- [48] V.G.Kostishyn, L.V.Panina, L.V.Kozhitov, A.V.Timofeev, and A.N.Kovalev, "Synthesis and Multiferroics properties of M-type SrFe<sub>12</sub>O<sub>19</sub> hexaferrite ceramics," *Journal of Alloys and Compounds*, vol. **645**, pp. 297-300 (2015).
- [49] J.Liu, J.Zhang, P.Zhang, SWang, C.Lu, Y.Li, and M.Zhang, "Tunable microwave absorbing properties of barium hexa-ferrite nano powders by surface carbonized layers," *Materials Letters*, vol. **158**, pp. 53-57(2015).
- [50] T.Li, Y.Li, R.Wu, H.Zhou, X.Fang, S.Su, A.Xia, C.Jin, and X.Liu, “A solution for the preparation of hexagonal M-type SrFe<sub>12</sub>O<sub>19</sub> ferrite using egg white: Structural and magnetic properties,” *Journal of Magnetism and Magnetic Materials*, vol. **393**, pp.325-330(2015).
- [51] F.Rhein, R.Karmazin, M.Krispin, T.Reimann, & O.Gutfleisch,, “ Enhancement of coercivity and saturation magnetization of Al<sup>3+</sup> substituted M-type Sr-hexaferrites,” *Journal of Alloys and Compounds*, vol. **690**, pp.979-985(2017)
- [52] P.Sivakumar, L.Shani, Y.Yeshurun, A.Shaulov, & A.Gedanken, “Facile sonochemical preparation and magnetic properties of strontium hexaferrite (SrFe<sub>12</sub>O<sub>19</sub>) nanoparticles,” *Journal of Materials Science. Materials in Electronics*, vol. **27**, no.6, pp. 5707-5714(2016).
- [53] S.B.Narang, A.Singh, and K.Singh, "High frequency dielectric behavior of rare earth substituted Sr-M hexaferrite," *Journal of Ceramic Processing Research*, vol. **8**, no.5, pp. 347 (2007).
- [54] B.D.Cullity, and S.R.Stock., "Elements of X-ray Diffraction, 3rd edn Prentice Hall." *New York* (2001).
- [55] V.N.Dhage, M.L.Mane, A.P.Keche, C.T.Birajdar, and K.M.Jadhav, "Structural and magnetic behavior of aluminium doped barium hexaferrite nanoparticles synthesized by solution combustion technique." *Physica B: Condensed Matter*, vol.**406**, no.4, pp. 789-793(2011).
- [56] S.Thongmee, T.Osotchan, P.Winotai, and I.M.Tang, "Fluctuations in the Local Fields Due to Al<sup>3+</sup> Ions Substitution in the M-Type Barium Hexaferrites, BaFe<sub>12</sub>-

$x\text{Al}_x\text{O}_{19}$ ." *International Journal of Modern Physics B* , vol.**12**, no.27-28, pp. 2847-2855 (1998).